

Spatio-temporal footprints of urbanisation in Surat, the Diamond City of India (1990–2009)

Richa Sharma · Aniruddha Ghosh ·
Pawan Kumar Joshi

Received: 14 February 2012 / Accepted: 5 July 2012 / Published online: 26 July 2012
© Springer Science+Business Media B.V. 2012

Abstract Urbanisation is a ubiquitous phenomenon with greater prominence in developing nations. Urban expansion involves land conversions from vegetated moisture-rich to impervious moisture-deficient land surfaces. The urban land transformations alter biophysical parameters in a mode that promotes development of heat islands and degrades environmental health. This study elaborates relationships among various environmental variables using remote sensing dataset to study spatio-temporal footprint of urbanisation in Surat city. Landsat Thematic Mapper satellite data were used in conjugation with geo-spatial techniques to study urbanisation and correlation among various satellite-derived biophysical parameters, [Normalised Difference Vegetation Index, Normalised Difference Built-up Index, Normalised Difference Water Index, Normalised Difference Bareness Index, Modified NDWI and land surface temperature (LST)]. Land use land cover was prepared using hierarchical decision tree classification with an accuracy of 90.4 % ($\kappa=0.88$) for 1990 and 85 % ($\kappa=0.81$) for 2009. It was found that the city has expanded over 42.75 km² within a decade, and these changes resulted in elevated surface temperatures. For example, transformation from vegetation to built-up has resulted in 5.5 ± 2.6 °C increase in land surface

temperature, vegetation to fallow 6.7 ± 3 °C, fallow to built-up is 3.5 ± 2.9 °C and built-up to dense built-up is 5.3 ± 2.8 °C. Directional profiling for LST was done to study spatial patterns of LST in and around Surat city. Emergence of two new LST peaks for 2009 was observed in N–S and NE–SW profiles.

Keywords Biophysical parameters · Expert classification · LST · LULC changes · Urbanisation

Introduction

Urbanisation is the most important anthropogenic activity after greenhouse gas emissions that impact climate (Kalnay and Cai 2003). Urbanisation on one hand benefits economic welfare of society; on the contrary, it threatens the biophysical health of the city itself. It causes detriment to environmental quality, including biodiversity (McKinney 2006; Delgado-V and French 2012; Threlfall et al. 2012), soil fertility (Chen 2007), water quality (Kaushal et al. 2008; Paul and Meyer 2001), and impacts other natural resources (Huang et al. 2010) along with ecosystem services (Alberti 2005; Bolund and Hunhammar 1999). Urban land transformations are most complex and dramatically irreversible land use changes and are thus one of the most studied phenomena (Wenhui 2012; Jiang and Tian 2010; Taubenböck et al. 2009; Souch and Grimmond 2006). Urban land use changes such as loss of vegetation (Scolozzi and Geneletti 2012), increased built-up and open areas (Ng et al. 2011) along

R. Sharma · A. Ghosh · P. K. Joshi (✉)
TERI University,
New Delhi, India 110070
e-mail: pkjoshi27@hotmail.com

with increased expanse of urban fabrics such as concrete and asphalt altogether alter the local climate of a city by modifying various biological and physical characteristics of the environment. These include vegetation cover, impervious built-up covers, presence of moisture, surface and air temperatures, soil properties and others, which in turn are governed by land use characteristics (Voogt and Oke 2003).

With urbanisation taking over the world at an unprecedented pace, Indian cities are no exception. By 2050, India is expected to inhabit 0.9 billion urban population with a projection from 29.7 % in 2009 to about 54.2 % by 2050 (UN 2010). Delhi, Mumbai and Kolkata already fall in the category of the mega-cities, and Chennai is soon going to join these along with Hyderabad and Bangalore (Joshi et al. 2011). Apart from megacities, a number of smaller urban agglomerations are showing tremendous growth since the past decade (Taubenböck et al. 2009). Surat, for instance, has great potential of transforming into a megacity. Surprisingly, not enough work has been done to study its urban sprawl and related impacts. The city has been expanding ever since 1951 when it had a population of 0.24 million that gradually increased to 0.49 in 1971, to 1.52 in 1991 and finally crossing 2.8 in 2001 and reaching 4.46 million in 2011 (Census of India 2011). It is expected to inhabit 5.57 million people by 2025 (UN 2010).

Land surface temperature (LST) is the most studied biophysical parameter related to urban health. It has a two-way relationship with environmental parameters as it influences some of them and in turn gets influenced by others. Some literature is available on former part of this interaction. Baur and Baur (1993) found that urbanisation-related changes in LST resulted in local extinction of land snails in Basel. Whitford et al. (2001) stated LST as one of the four ecological performance indicators. LST also directly impacts surface energy budget (Bastiaanssen et al. 1998) and thus influences air temperature of the area. This results in emergence of two types of urban heat Islands (UHI) in same area, viz., surface UHI and atmospheric UHI. This paper examines formal half of LST and environment interaction using satellite-derived equivalents of various parameters. This study thus employs remote sensing to demonstrate how different environmental parameters like vegetation cover and health, moisture intensity and bareness influence LST.

With the advent of geospatial technology, it has become possible to remotely monitor the biophysical variables and changing land use patterns and to analyse their interactions (Buyantuyev and Wu 2012). Though a number of studies have been carried out to examine the variability among greenness, surface temperature (Son et al. 2012; Julien and Sobrino 2009; Reynolds et al. 2008; Julien et al. 2006; Weng et al. 2004; Sandholt et al. 2002; Owen et al. 1998; Gillies et al. 1997; Goetz 1997) and land use associations (Amiri et al. 2009; Zhou et al. 2011; Jiang and Tian 2010; Xiao et al. 2008; Xiao and Weng 2007), little work has been done in assessing the variability of other biophysical factors in context to LST (Uddin et al. 2010; Chen et al. 2006). Limited research material could be found on the relationship of these parameters with respect to each other and how this relationship differs for different land uses. Uddin et al. (2010) and Chen et al. (2006) have attempted classification using four main indices, viz., Normalised Difference Vegetation Index (NDVI), Normalised Difference Water Index (NDWI), Normalised Difference Built-up Index (NDBI) and Normalised Difference Bareness Index (NDBaI). In the present study, an additional modified water index was developed, Modified Normalised Water Index (MNDWI), for extracting water. All these factors were considered as these could account to assess spatio-temporal footprints of urbanisation.

Surat—the Diamond City

Surat city is the commercial capital city of Gujarat (India) and also serves as administrative capital of Surat district. It is situated on the banks of Tapi river which perennially flows northeast to southwest finally joining the Arabian Sea, situated 22 km west to the city. The city is situated at 21.25° N and 72.87° E (Fig. 1). The region experiences hot summers with temperature ranging from 38 to 45 °C. Winters are mild, but the months of December and January are coldest with temperatures varying between 10 and 15.5 °C. The average annual rainfall is 1,143 mm (Surat Municipal Corporation 2011).

Being a commercial hub, the region has witnessed tremendous urbanisation over the past few decades. It ranks 36th in the list of the world's largest cities with a population of over 2.5 million

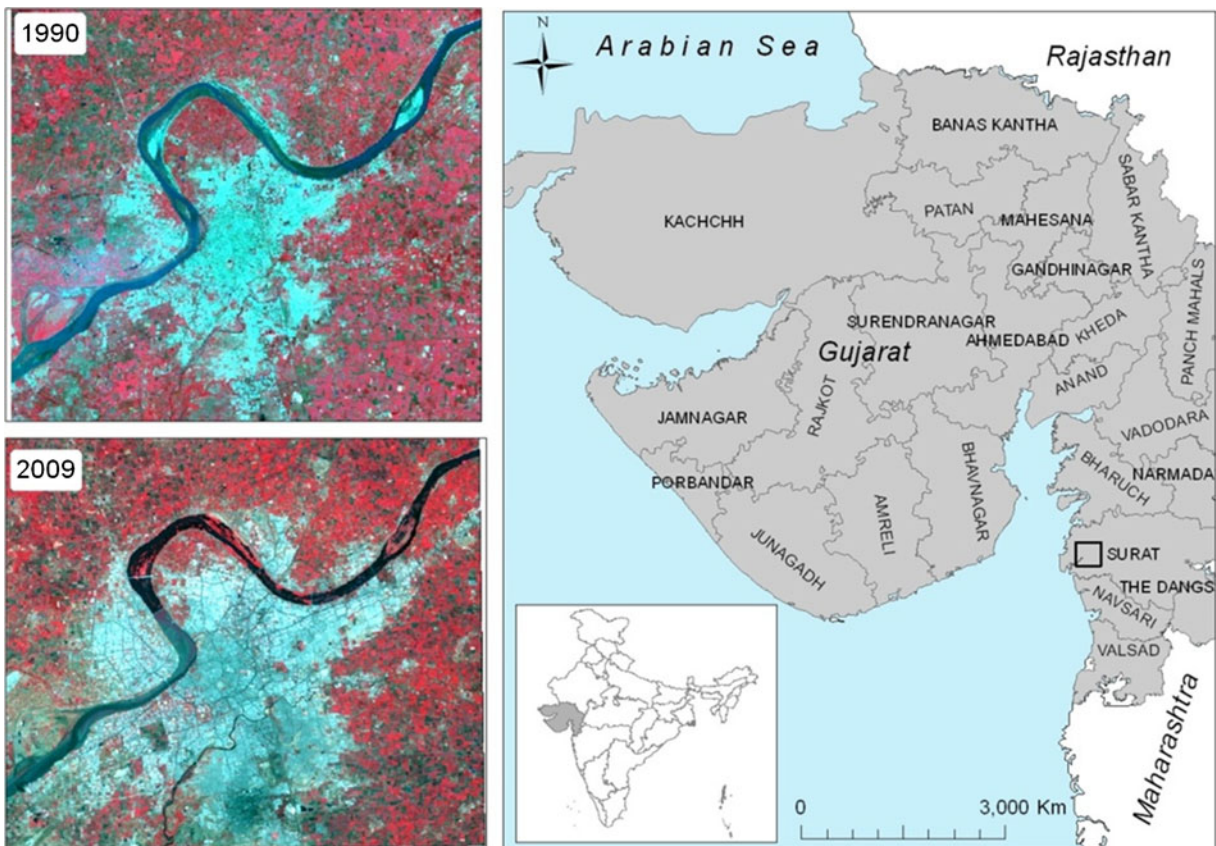


Fig. 1 Location of the study area

in 2001 (population density of 1,376 persons/km²) and the third cleanest metropolitan region in India. The city has total population of more than 6 million of which 80 % is urban population and the remaining 1.24 million is rural (Census of India 2011). Surat has immense business and job opportunities that trigger high immigration rates to the city resulting in increased population. The two major economic activities are agriculture and diamond cutting. A large number of small-scale diamond cutting industries have given the name ‘Diamond City’ to this place.

The study area extends spatially from 21.29° N and 21.12° N to 72.74° E and 72.94° E, spanning across 386.28 km² covering the city (city limits of 326 km²) and peripheral urban–rural fringe. The study area mainly falls in the Chorasi taluk of Surat district but also covers parts of adjoining taluks of Olpad in the north, Kamrej in the east and Palsana in the south-east. It is bound by Navsari on the south.

Materials and methods

Satellite data

Landsat 5/4 Thematic Mapper (TM) satellite images (Path/Row, 148/45) dated October 19, 1990 and October 23, 2009 were used. Landsat is a medium-resolution (30 and 120 m) data with seven bands that are most commonly used for environmental studies. Landsat TM data consist of seven bands of which the first three are visible bands, the fourth is near-infrared, bands five and seven fall in shortwave infrared regions and sixth is the thermal band. The geometrically and radiometrically corrected images rectified to a common Universal Transverse Mercator were procured from the USGS Earth Resource Observation Systems Data Center. The details and characteristics of the satellite data used are given in Table 1.

Spectral enhancement was done using band ratioing to compute various indices. This performed a twofold

Table 1 Landsat 5 TM sensor system characteristics

Band	Spectral details; wavelength (μm)	Spatial resolution (m)	Applications
TM1	Blue (0.45–0.52)	30	Can penetrate water bodies, thus help in coastal water studies, identifying cultural features
TM2	Green (0.52–0.6)	30	Studying water turbidity, vegetation studies
TM3	Red (0.63–0.69)	30	Monitoring vegetation health
TM4	Near-infrared (0.76–0.9)	30	Studying land–water and cropped–non-cropped lands, identifying crops
TM5	Shortwave infrared (1.55–1.75)	30	Cloud and snow studies, studying geological features, monitoring vegetation moisture
TM6	Thermal infrared (10.40–12.5)	120	Surface temperature studies, LST estimation, vegetation stress studies
TM7	Shortwave infrared (2.08–2.35)	30	Studying vegetation moisture content, studying rocks and minerals

function: *firstly*, these served as variables in classification, and *secondly*, these were used to study dynamics of different biophysical parameters (viz., greenness, wetness, bareness and built-up intensity) with respect to

each other and that to thermal response of environment. Red (TM 3) and infrared (TM4) bands helped to enhance greenness (Maxwell and Sylvester 2012; Purevdorj et al. 1998), infrared (TM4) and shortwave

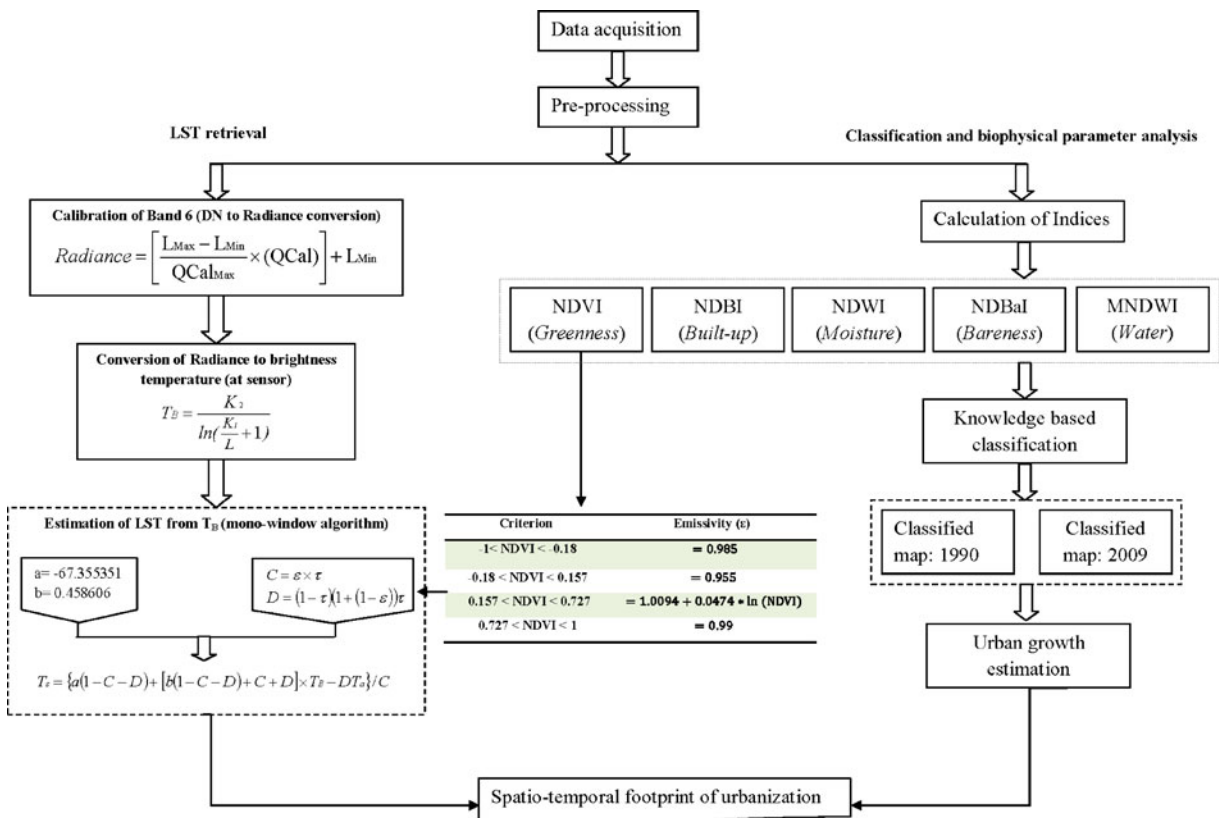


Fig. 2 Flowchart describing methodology. (Where, L_{Max} and L_{Min} (watts per square metre per steradian per micrometre) are spectral radiances for thermal band (band 6) at digital numbers 1 and 255, respectively, i.e. QCal_{Min} and QCal_{Max} values, while QCal represents the DN value; K_1 ($607.76 \text{ W}/(\text{m}^2/\text{sr}\cdot\mu\text{m})$) and

K_2 (1260.56 K) are pre-launch satellite calibration constants; a and b are constants; T_a refers to effective mean atmospheric temperature, and C and D are computed using emissivity and atmospheric transmittance derived from water vapour (grams per square centimetre), where ε is emissivity and τ is transmittance)

Table 2 Description of various image transformation used with references

Transformation	Algorithm	Application	References
NDVI	$\frac{\rho_4 - \rho_3}{\rho_4 + \rho_3}$	Vegetation studies (fractional vegetation cover, leaf area index, plant phenology, productivity, and chlorophyll density), forest cover estimation, canopy studies, studying rainfall patterns, drought monitoring, estimating biomass, studying urbanisation, as surface urban heat islands (SUHI) indicator	Anyamba and Tucker (2005); Weiss et al. (2004); Zhou et al. (2004); Gallo et al. (1995); Carlson and Ripley (1997); Jong et al. (2011); Yuan and Bauer (2007); Li and Fox (2012).
NDBI	$\frac{\rho_5 - \rho_4}{\rho_5 + \rho_4}$	Extraction of built-up areas and to study SUHI	Zha et al. (2003); Zhang et al. (2009).
NDWI	$\frac{\rho_4 - \rho_5}{\rho_4 + \rho_5}$	Used in vegetation studies as it gives an indication of vegetation liquid	Gao (1996); Gabor and Jombach (2009); Maki et al. 2004)
NDBaI	$\frac{\rho_5 - \rho_6}{\rho_5 + \rho_6}$	Extraction of bare areas that are moisture deficient	Chen et al. (2006)
MNDWI	$\frac{\rho_1 - \rho_2}{\rho_1 + \rho_2}$	Mapping areas covered by water	Introduced ^a

^a This index is introduced in this paper

infrared (TM5) were used to enhance built-up areas (Bridhikitti and Overcamp 2012; Ma et al. 2010; Zhang et al. 2009) and enhance canopy vegetation water content (Jackson et al. 2004; Serrano et al. 2000; Gao 1996). Shortwave infrared (TM5) and thermal infrared (TM6) were employed for enhancing bare lands (Nasipuri and Chatterjee 2009). LST retrieval was performed using thermal information of TM6 band. For more accurate mapping and extraction of water bodies from image, MNDWI was computed by transforming blue (TM1) and shortwave infrared (TM5) bands. Figure 2 briefly describes the methodology followed.

Data processing

Estimating biophysical parameters

NDVI, NDBI and MNDWI were used to map land use and land cover (LULC) classes. These metrics along

with NDBaI and NDWI were used to investigate correlation of various biophysical parameters (intensity of moisture, greenness, build-up density and extent of bareness) with that of thermal response of urbanised areas in contrast to vegetated areas. Table 2 presents a brief review of various indices used, their computation and uses along with references.

Land surface temperature retrieval

Landsat TM band 6 has been extensively exploited to study thermal dynamics of various earth surface features (Qin et al. 2001; Schott et al. 2001). LST was derived using thermal infrared (TM6) band (10.40–12.50 μm), with effective wavelength of 11.457 μm, has relatively lower radiometric sensitivity and coarser spatial resolution of 120×120 m. Qin et al. (2001) mono-window algorithm (Sun et al. 2010) was used to retrieve LST from thermal DN values, and NDVI was used here for emissivity correction to obtain final LST images.

Table 3 Hypothesis, rules and variables for 1990 and 2009 satellite images

Hypothesis	Rules	Conditions
Built-up	Built-up areas and rooftops	NDVI <0.02 and NDWI <0.2 AND NDBI ≥0.15 AND NDBaI <-0.25
Sediment	Riverbed, silt and sandy	-0.75 ≤NDBaI ≤-0.6
Vegetation	Agriculture and urban green	NDVI >0.3 and 0 <NDWI <0.3 AND -0.6 <NDBaI <0.3 and -0.2 <NDBI <-0.02
Water body	Rivers and water bodies	MNDWI ≥0.3
Fallow land	Agricultural fallow	NDVI <0.2 and -0.25 ≤NDWI <-0.1 and NDBaI ≤-0.3 and 0.1 <NDBI <0.3

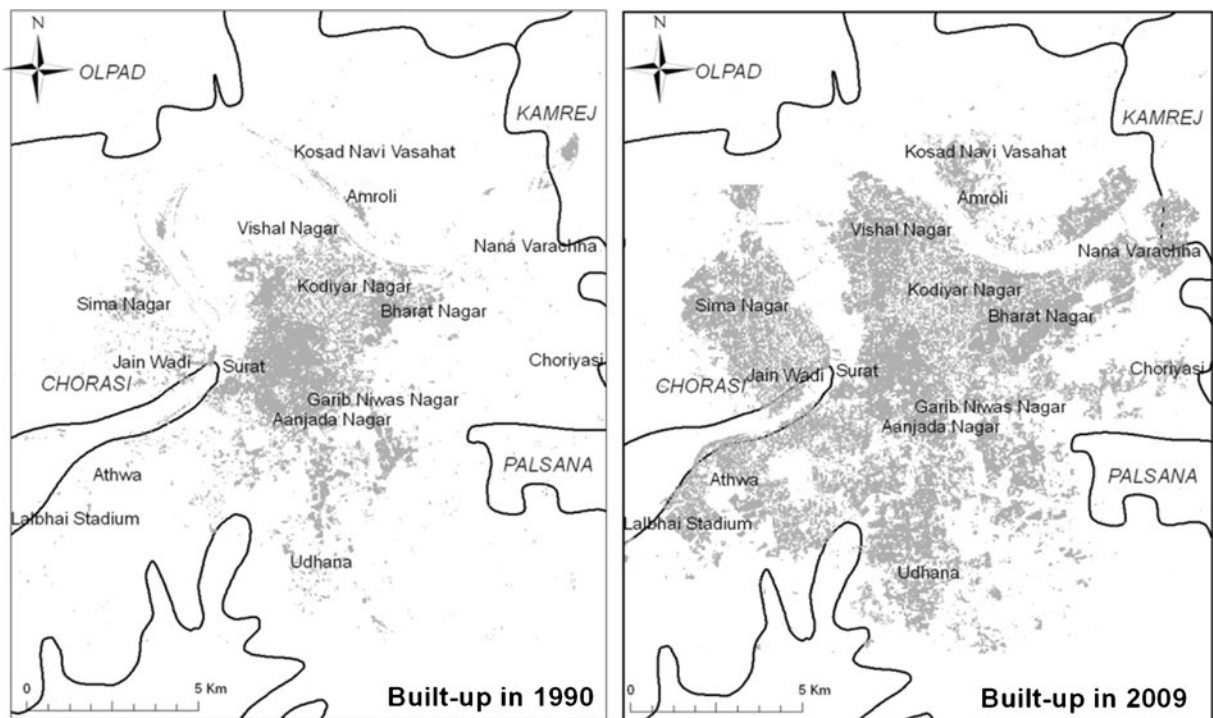


Fig. 3 Expansion in built-up from 1990 to 2009

Characterising land use patterns

Five broad categories of LULC were identified based on visual image interpretation keys; (1) *Built-up* comprised of urban features and impervious structures like asphalt and concrete roads; (2) *River bed* included sediments along river and other sandy and silt deposition structures; (3) A broad

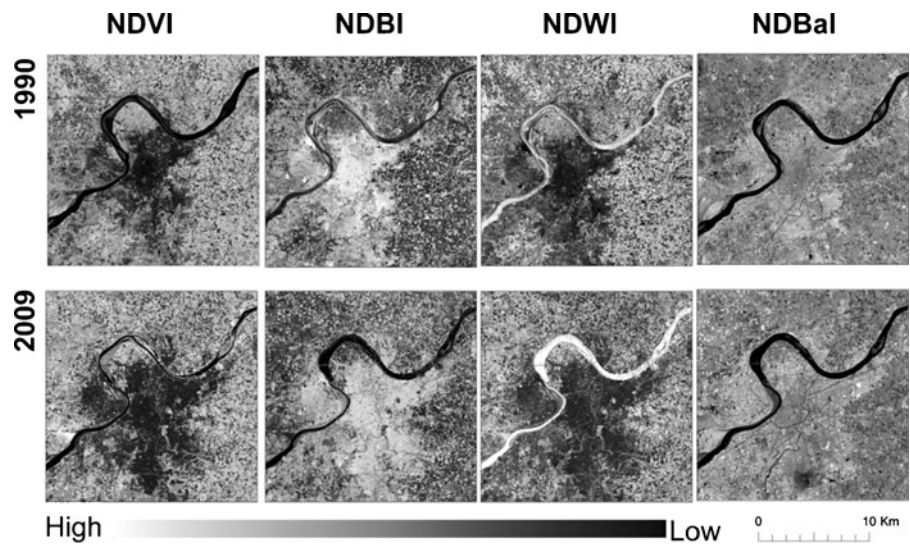
class named '*Vegetation*' included land under agriculture as well as urban vegetation and other canopy; (4) Agricultural land without any vegetation cover including agricultural fallow was classified as *Fallow land*; and (5) *Water body* covered Tapi river and other small water storage tanks.

Knowledge-based classification technique was employed to categorise satellite images into LULC classes. It is a type of hierarchical decision tree algorithm based on hypothesis testing that evaluates various rules and conditions defined by the user. Rules are condition (IF) and action (THEN) statements. Hypothesis, rules and condition represented in linear dendritic decision tree are inferred and processed to generate outputs (Table 3). Indices computed earlier were fed into knowledge engineer as variables for different LULC classes (the hypothesis), and their threshold values defined the rules for each hypothesis. Due to high efficiency of MNDWI in identifying water pixels, it was used alone for water extraction. The decision tree thus generated was executed to map LULC. To assess the classification accuracy, 150 randomly

Table 4 Accuracy assessment for 1990 and 2009 classification

Class name	1990			2009		
	PA (%)	UA (%)	Kappa	PA (%)	UA (%)	Kappa
Built-up	90.2	92	0.90	80.39	82	0.77
Sediment	86.27	88	0.85	77.59	90	0.87
Vegetation	90.2	92	0.90	88.24	90	0.87
Water	93.88	92	0.90	90.91	80	0.76
Fallow	91.67	88	0.85	86.96	80	0.76
Overall	90.4		0.88	84.4		0.8050

Fig. 4 Biophysical parameters in 1990 and 2009 (NDWI, NDVI, NDBI and NDBaI)



generated points were overlaid on the satellite image. Statistically valid sampling strategy was adopted to assess commission, omission and overall accuracy (Stehman 1996).

Statistical analysis

Biophysical parameters

Urban land transformations have great impacts on the biophysical health of the environment. To examine the complexity and dynamics of this relationship, 150 experimental and 150 control points were randomly generated. All the points were well distributed among the LULC classes and the entire study area. At least 30 points per LULC were generated to extract values of each of the parameters under study. These were then used to mine out the values of biophysical parameters two times for analysing the influence of LULC change on the biophysical environment. Correlation and regression techniques were employed to exemplify how the environment responds to stimulus of urbanisation.

Directional profiles of LST

Based on the spatial patterns of urban expansion in the area, four directional profiles for LST were selected: north–south (N–S), east–west (E–W), northeast–

southwest (NE–SW) and northwest–southeast (NW–SE) profiles. LST values for these spatial profiles were analysed across the background of expansion in the built-up area over the study period.

Results and discussion

LULCC analysis

1990 and 2009 LULC maps were analysed to study expansion of urban area. The classes mapped were built-up, vegetation, fallow, river bed and water. Area statistics for LULC ascertained massive expansion (nearly three times) in urban expanse at the cost of vegetation and fallow lands. The urban extent increase has been equal to 42.74 km² from 1990 to 2009. With improved connectivity through roads, highways and bridges, the city has expanded in almost all directions (Fig. 3) resulting in newer settlements in Amroli, Nana Varachha, Choriyasi, Athwa, Vishal Nagar, Sima Nagar and Jain Wadi. Udhana has been the centre for highly denser sprawls that could be attributed to its high economic importance for diamond cutting and polishing works. Overall classification accuracy of LULC map for 1990 was 90.4 % and for 2009 was 84.4 % (Table 4). The expert classification accuracy is remarkably good as compared to hard classification methods (Punia et al. 2011; Wentz et al. 2008). Due to

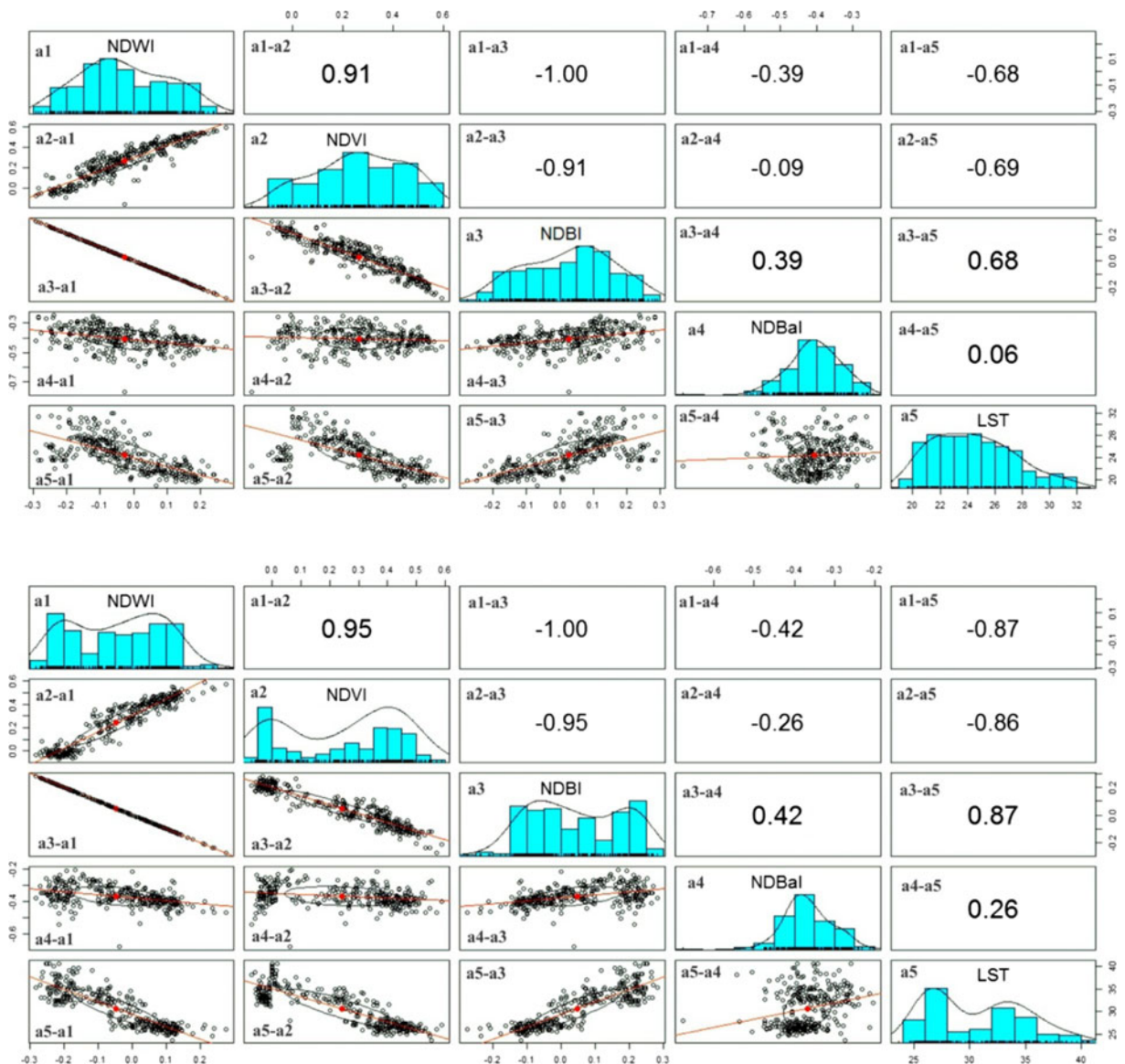


Fig. 5 Scatter plots and coefficient of determination for different parameters in 1990 and 2009

similar spectral responses of long fallow and less dense built-up areas, 2009 image has poorer accuracy for fallow and built-up classes.

Analysis of biophysical parameters

For quantification of relationship between biophysical parameters under study (Fig. 4), correlation analysis was carried out using 300 point values. The analysis demonstrated that LST shoots up with a fall in NDVI or greenness. A similar relationship was observed for

NDWI also. Lesser will be the water content, lesser will be evaporation and hence reduced cooling will result in higher temperature. This explanation also supports a positive correlation between NDVI and NDWI (Fig. 5). NDBI represents built-up intensity of land. The higher the built-up intensity, the more impervious and the lower the moisture content. Thus, LST–NDBI behaves asynchronously. NDBI and NDWI exhibited a perfectly negative relationship as the two indices have exactly the same numerical values but antonymous signs.

Bareness index did not exhibit a strong correlation with any of the parameters. Similar results have been observed by Essa et al. (2012). NDBaI exemplified a negative correlation with NDVI and NDWI and a positive one with LST and NDBI for both years. But this relationship shows inconsistency when analysed separately for control and experimental points showing positive values for year 1990 (0.032 for control and 0.183 for experimental) and negative for year 2009 (−0.09 for control and −0.20671 for experimental). Uddin et al. (2010) also state that in some isolated cases, NDBaI and LST have a positive variability with respect to each other (Fig. 5).

LST characterisation

Experimental and control point values of LST were analysed to assess thermal response of different LULC classes. The average temperature of experimental built-up points is relatively higher than that for vegetation areas. LST for vegetation to built-up change areas increased by 8.8 ± 2.6 °C, and fallow land to built-up increased by 6.6

± 2.8 °C, while 8.6 ± 2.8 °C change was observed for increase in built-up density.

Increase in average temperature for unchanged vegetated areas was assessed using control points and was found to be 3.3 ± 3.4 °C. Hence, the net increase in the temperature for changes from vegetation to built-up is around 5.5 ± 2.6 °C, vegetation to fallow is 6.7 ± 3 °C, fallow land to built-up is 3.5 ± 2.9 °C and built-up to dense built-up is 5.3 ± 2.8 °C. Temperature change for vegetation to fallow is higher than vegetation to built-up which could be due to land being fallow for long and thus being deficient in moisture. Also, as compared to fallow land, which is completely bare, built-up areas are characterised by shadow effects from building structures.

Temporal analysis of LST demonstrated that built-up areas have a higher temperature as compared to vegetation thus forming the foundation for phenomenon of urban heat island in the area (Schwarz et al. 2012; Liu and Zhang 2011) (Fig. 6). Built-up areas that have come up by replacing vegetation show elevated temperatures as compared to other areas. Urban areas contain impervious surfaces that decrease local

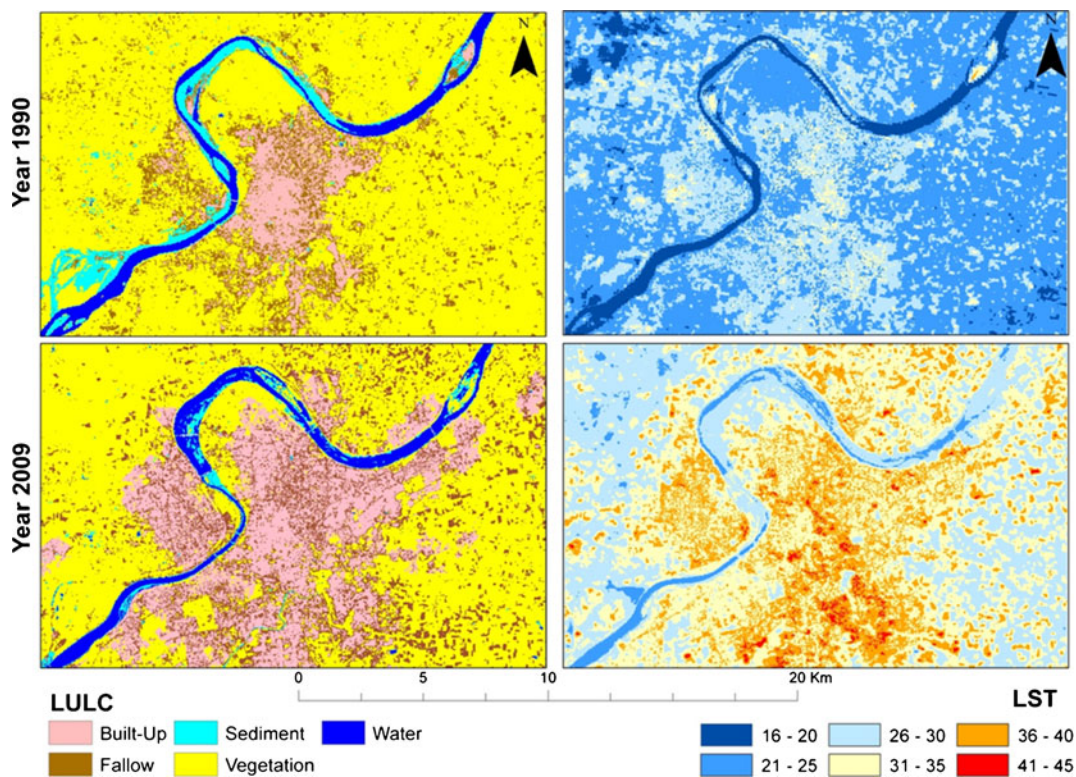


Fig. 6 LULC and LST for 1990 and 2009

infiltration, percolation and soil moisture (Brun and Band 2000). Due to their thermal properties, heat island phenomenon is triggered. LST is one of the key factors that control physical, chemical and biological processes in the environment and in turn is governed by them. Urbanisation in particular changes the thermal environment due to physical properties of its urban fabric (Pu et al. 2006) and encourages the development of urban heat island.

Spatial profile analysis

For a detailed analysis of spatial distribution of LST in the study area, four directional profiles were studied (Fig. 7). The profiles were constructed based on directions in which built-up area has expanded. N–S profile ran from Kosam and Sherdi villages in north of the river to Udhana industrial centre, in south of Surat city. Spatial N–S profile of LST for 1990 and 2009 improved our understanding that industrialised area

increased thermal environment. The curve became flatter for Surat city in 2009, and new peaks were observed in Udhana centre which were not there in 1990. This could be explained based on the expansion of built-up in Udhana area. E–W profile starts with agricultural lands of Bhesan and Melgama villages, passing built-up area of Jain Wadi crossing the river to industrial areas of Bharat Nagar, through the city of Surat, and finally ending in the agricultural lands of Kosmada and Ladvi villages. E–W profile exhibited results similar to N–S profile with low thermal response of agriculture. In 1990, only one major peak was observed in built-up area in and around Surat, while in 2009, profile flattened with higher temperature values illustrating impacts of increased built-up on LST.

The NW–SE profile sets out from agricultural areas of Talad and Sarol Gam villages; crossing across the river, it passes through Katargam, Surat and Shakti Nagar areas finally terminating through agricultural

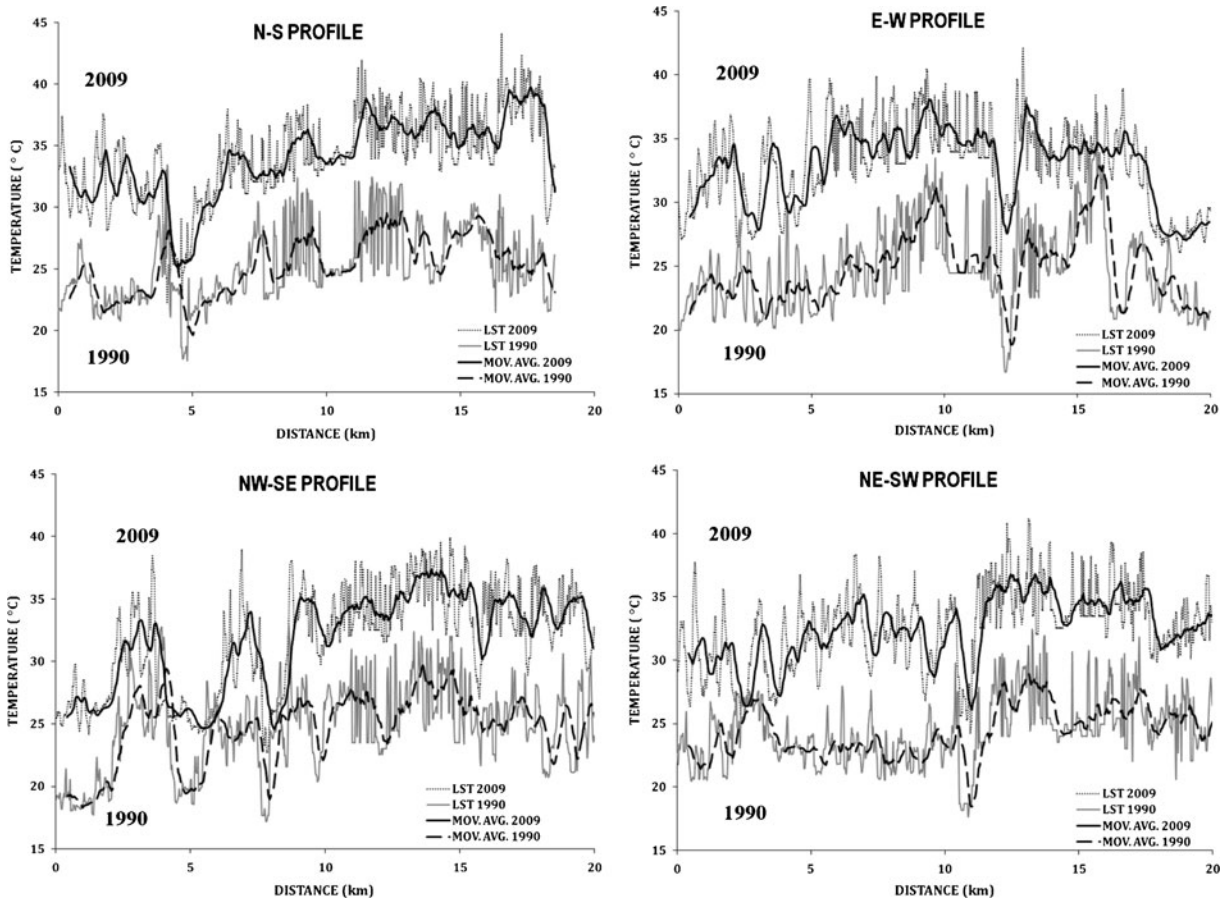


Fig. 7 Directional profiling of LST distribution in 1990 and 2009

areas of Bonand and Kharsava villages. Temperature values (Fig. 7) for agricultural areas, in the beginning and end of the profile, were generally lower with sporadic peaks due to fallow land. Built-up areas of Katargam, Surat and Shakti Nagar gave high temperature responses. Profile corresponding to river showed a steep depression in temperature. Such an observation was recorded for all four profiles regarding encountering river in between. NE–SW profile begins at fields of Abrama crossing the river passing through Kodyar Nagar and Surat city through Krishnaganj and Athwa to Vesu village. A peak was observed for the new built-up in 2009, towards the northern bank of the river. In 1990, fewer peaks were observed for Surat, Kishanganj and Athawa areas, but more and higher peaks were observed in 2009.

Conclusion

The study was taken up to assess spatio-temporal footprints of urbanisation in Surat city. Over a span of two decades, the city has spread over an area of 42.75 km², with multi-directional expansion of its built-up. The city has densely spread to the south in Udhana industrial hub and comparatively less dense northward spreads in Amroli and Kosad Navi Vasahat. Choriyasi, a small satellite town, manifests the eastward spread of the city, while Athawa manifested the same for the southwestern spreads. Older parts of Sima Nagar and Jain Wadi served as centres of urban growth for the west.

The urban expansion has altered the state of various biophysical parameters (including surface temperatures, moisture contents and vegetation cover) which govern the health of the environment. In this study, we qualitatively studied the multifaceted interactions of biophysical parameters and quantified relationships among them. The selected parameters retrieved from satellite data are LST (thermal behaviour of surface), NDVI (intensity of greenness), NDBI (intensity of built-up), NDWI (moisture status of surface) and NDBaI (bareness). Of these, LST–NDVI and LST–NDWI were found to vary inversely, while LST–NDBI and NDVI–NDWI had a strong positive correlation. Of these, NDBaI was one parameter that could not give consistent results and was characterised by very weak correlations with the other parameters. Although NDBaI has been successfully employed by Chen et al. (2006), in this work, some inconsistent results were obtained for this index. Thus,

we found that this index gave site-specific results, and there is further scope of developing a more robust index to measure the bareness intensity of the earth surface.

In face of urban heat island (UHI), LST parameter was more intensely analysed with respect to its changing spatial distribution against the background of changing LULC patterns. LST through UHI can have severe impacts on human and environmental health by increasing the frequency and intensity of heat waves (Tan et al. 2010). It was observed that with southward expansion of Udhana industrial area, new peaks for LST came up in 2009. Similar results were found for Athwa, Jain Wadi and Surat city areas. Apart from urban areas, some peaks came up for agricultural fallow lands.

Global urbanisation needs accurate information on the expansion of impervious surfaces and associated parameters. The parameters discussed in this study are of prime importance to assess the impact of urbanisation-linked development. Eco-planning in urban sector could use such information to achieve the goals of sustainable practices and planning. The information generated can also aid in understanding the contribution of local effects on the global phenomena of climate change and associated changes. These should be explored to understand the health of urban ecosystem and linkages with human well-being.

Acknowledgments The authors are thankful to anonymous reviewers for the suggestions. RS and PKJ thank the Department of Science and Technology (DST), Ministry of Science and Technology, Government of India, and AG acknowledges the Council of Scientific and Industrial Research (CSIR), Government of India for the support.

References

- Alberti, M. (2005). The effects of urban patterns on ecosystem function. *International Regional Science Review*, 28, 168–192.
- Amiri, R., Weng, Q., Alimohammadi, A., & Alavipanah, S. K. (2009). Spatial-temporal dynamics of land surface temperature in relation to fractional vegetation cover and land use/cover in the Tabriz urban area, Iran. *Remote Sensing of Environment*, 113, 2606–2617.
- Anyamba, A., & Tucker, C. J. (2005). Analysis of Sahelian vegetation dynamics using NOAA-AVHRR NDVI data from 1981–2003. *Journal of Arid Environments*, 63, 596–614.
- Bastiaanssen, W. G. M., Menenti, M., Feddes, R. A., & Holtlag, A. A. M. (1998). A remote sensing surface energy balance algorithm for land (SEBAL) 1. Formulation. *Journal of Hydrology*, 212–213, 198–212.

- Baur, B., & Baur, A. (1993). Climatic warming due to thermal radiation from an urban area as possible cause for the local extinction of a land snail. *Applied Ecology*, *30*, 333–340.
- Bolund, P., & Hunhammar, S. (1999). Ecosystem services in urban areas. *Ecological Economics*, *29*, 293–301.
- Bridhikitti, A., & Overcamp, T. J. (2012). Estimation of Southeast Asian rice paddy areas with different ecosystems from moderate-resolution satellite imagery. *Agriculture, Ecosystems and Environment*, *146*, 113–120.
- Brun, S. E., & Band, L. E. (2000). Simulating runoff behavior in an urbanizing watershed. *Computers, Environment and Urban Systems*, *24*, 5–22.
- Buyantuyev, A., & Wu, J. (2012). Urbanization diversifies land surface phenology in arid environments: interactions among vegetation, climatic variation, and land use pattern in the Phoenix metropolitan region, USA. *Landscape and Urban Planning*, *105*, 149–159.
- Carlson, T. N., & Ripley, D. A. (1997). On the relation between NDVI, fractional vegetation cover, and leaf area index. *Remote Sensing of Environment*, *62*, 241–252.
- Census of India (2011). Government of India.
- Chen, J. (2007). Rapid urbanization in China: a real challenge to soil protection and food security. *Catena*, *69*, 1–15.
- Chen, X.-L., Zhao, H.-M., Li, P.-X., & Yin, Z.-Y. (2006). Remote sensing image-based analysis of the relationship between urban heat island and land use/cover changes. *Remote Sensing of Environment*, *104*, 133–146.
- Delgado-V, C. A., & French, K. (2012). Parasite-bird interaction in urban areas: Current evidence and emerging questions. *Landscape and urban planning*, *105*, 5–14.
- Essa, W., et al. (2012). Evaluation of the DisTrad thermal sharpening methodology for urban areas. *International Journal of Applied Earth Observation and Geoinformation*, *19*, 163–172.
- Gabor, P., & Jombach, S. (2009). The relationship between the biological activity and the land surface temperature in Budapest. *Applied Ecology and Environmental Research*, *7*, 241–251.
- Gallo, K. P., Tarpley, J. D., McNab, A. L., & Karl, T. R. (1995). Assessment of urban heat islands: a satellite perspective. *Atmospheric Research*, *37*, 37–43.
- Gao, B. (1996). NDWI—a normalized difference water index for remote sensing of vegetation liquid water from space. *Remote Sensing of Environment*, *58*, 257–266.
- Gillies, R. R., et al. (1997). A verification of the ‘triangle’ method for obtaining surface soil water content and energy fluxes from remote measurements of the Normalized Difference Vegetation Index (NDVI) and surface radiant temperature. *International Journal of Remote Sensing*, *18*, 3145–3166.
- Goetz, S. J. (1997). Multi-sensor analysis of NDVI, surface temperature and biophysical variables at a mixed grassland site. *International Journal of Remote Sensing*, *18*, 71–94.
- Huang, S. L., Yeh, C. T., & Chang, L. F. (2010). The transition to an urbanizing world and the demand for natural resources. *Current Opinion in Environmental Sustainability*, *2*(3), 136–143.
- Jackson, T. J., et al. (2004). Vegetation water content mapping using Landsat data derived normalized difference water index for corn and soybeans. *Remote Sensing of Environment*, *92*, 475–482.
- Jiang, J., & Tian, G. (2010). Analysis of the impact of land use/land cover change on land surface temperature with remote sensing. *Procedia Environmental Sciences*, *2*, 571–575.
- Jong, R., et al. (2011). Analysis of monotonic greening and browning trends from global NDVI time-series. *Remote Sensing of Environment*, *115*, 692–702.
- Joshi, P. K., Bairawa, B. M., Sharma, R., & Sinha, V. S. P. (2011). Assessing urbanization patterns over India using temporal DMSP-OLS night time satellite data. *Current Science*, *100*, 1479–1482.
- Julien, Y., & Sobrino, J. A. (2009). The Yearly Land Cover Dynamics (YLCD) method: an analysis of global vegetation from NDVI and LST parameters. *Remote Sensing of Environment*, *113*, 329–334.
- Julien, Y., Sobrino, J. A., & Verhoef, W. (2006). Changes in land surface temperatures and NDVI values over Europe between 1982 and 1999. *Remote Sensing of Environment*, *103*, 43–55.
- Kalnay, E., & Cai, M. (2003). Impact of urbanization and land-use change on climate. *Nature*, *423*, 528–531.
- Kaushal, S., et al. (2008). Interaction between urbanisation and climate variability amplifies watershed nitrate export in Maryland. *Environmental Science and Technology*, *42*, 5872–5878.
- Li, Z., & Fox, J. M. (2012). Mapping rubber tree growth in mainland Southeast Asia using time-series MODIS 250 m NDVI and statistical data. *Applied Geography*, *32*, 420–432.
- Liu, L., & Zhang, Y. (2011). Urban heat island analysis using the Landsat TM data and ASTER data: a case study in Hong Kong. *Remote Sensing*, *3*, 1535–1552.
- Ma, Y., Kuang, Y., & Huang, N. (2010). Coupling urbanization analyses for studying urban thermal environment and its interplay with biophysical parameters based on TM/ETM+ imagery. *International Journal of Applied Earth Observation and Geoinformation*, *12*, 110–118.
- Maki, M., Ishihara, M., & Tamura, M. (2004). Estimation of leaf water status to monitor the risk of forest fires by using remotely sensed data. *Remote Sensing of Environment*, *90*, 441–450.
- Maxwell, S. K., & Sylvester, K. M. (2012). Identification of “ever-cropped” land (1984–2010) using Landsat annual maximum NDVI image composites: Southwestern Kansas case study. *Remote Sensing of Environment*, *121*, 186–195.
- Mckinney, M. L. (2006). Urbanization as a major cause of biotic homogenization. *Biological Conservation*, *127*, 247–260.
- Nasipuri, P., & Chatterjee, A. (2009). Land use around Maithon reservoir: a study from high-resolution ASTER data. *Current Science*, *97*, 25–27.
- Ng, C. N., Xie, Y. J., & Yu, X. J. (2011). Measuring the spatio-temporal variation of habitat isolation due to rapid urbanization: a case study of the Shenzhen River cross-boundary catchment, China. *Landscape and Urban Planning*, *103*, 44–54.
- Owen, T. W., Carlson, T. N., & Gillies, R. R. (1998). An assessment of satellite remotely-sensed land cover parameters in quantitatively describing the climatic effect of urbanization. *International Journal of Remote Sensing*, *19*, 1663–1681.
- Paul, M. J., & Meyer, J. L. (2001). Streams in the urban landscape. *Annual Review of Ecology and Systematics*, *32*, 333–365.
- Pu, R., Gong, P., Michishita, R., & Sasagawa, T. (2006). Assessment of multi-resolution and multi-sensor data for urban surface temperature retrieval. *Remote Sensing of Environment*, *104*, 211–225.

- Punia, M., Joshi, P. K., & Porwal, M. C. (2011). Decision tree classification of land use land cover for Delhi, India using IRS-P6 AWiFS data. *Expert Systems with Applications*, 38, 5577–5583.
- Purevdorj, T., Tateishi, R., Ishiyama, T., & Honda, Y. (1998). Relationships between percent vegetation cover and vegetation indices. *International Journal of Remote Sensing*, 19, 3519–3535.
- Qin, Z., Karnieli, A., & Berliner, P. (2001). A mono-window algorithm for retrieving land surface temperature from Landsat TM data and its application to the Israel–Egypt border region. *International Journal of Remote Sensing*, 22, 3719–3746.
- Raynolds, M. K., Comiso, J. C., Walker, D. A., & Verbyla, D. (2008). Relationship between satellite-derived land surface temperatures, arctic vegetation types, and NDVI. *Remote Sensing of Environment*, 112, 1884–1894.
- Sandholt, I., Rasmussen, K., & Anderson, J. (2002). A simple interpretation of the surface temperature/vegetation index space for assessment of surface moisture status. *Remote Sensing of Environment*, 79, 213–224.
- Schott, J. R., et al. (2001). Calibration of Landsat thermal data and application to water resource studies. *Remote Sensing of Environment*, 78, 108–117.
- Schwarz, N., Schlink, U., Franck, U., & Grobmann, K. (2012). Relationship of land surface and air temperatures and its implications for quantifying urban heat island indicators—an application for the city of Leipzig (Germany). *Ecological Indicators*, 18, 693–704.
- Scolozzi, R., & Geneletti, D. (2012). A multi-scale qualitative approach to assess the impact of urbanization on natural habitats and their connectivity. *Environmental Impact Assessment Review*, 36, 9–22.
- Serrano, L., et al. (2000). Deriving water content of chaparral vegetation from AVIRIS data. *Remote Sensing of Environment*, 74, 570–581.
- Son, N. T., et al. (2012). Monitoring agricultural drought in the Lower Mekong Basin using MODIS NDVI and land surface temperature data. *International Journal of Applied Earth Observation and Geoinformation*, 18, 417–427.
- Souch, C., & Grimmond, S. (2006). Applied climatology: urban climate. *Progress in Physical Geography*, 30, 270–279.
- Stehman, S. V. (1996). Estimation of Kappa coefficient and its variance using stratified random sampling. *Photogrammetric Engineering and Remote Sensing*, 26, 401–407.
- Sun, Q., Tan, J., & Xu, Y. (2010). An ERDAS image processing method for retrieving LST and describing urban heat evolution: a case study in the Pearl River Delta Region in South China. *Environmental Earth Sciences*, 59, 1047–1055.
- Surat Municipal Corporation (2011). *Surat Municipal Corporation*, <http://www.suratmunicipal.org> [Online]. Surat Municipal Corporation. Accessed 27 July 2012.
- Tan, J., et al. (2010). The urban heat island and its impact on heat waves and human health in Shanghai. *International Journal of Biometeorology*, 54, 75–84.
- Taubenböck, H., et al. (2009). Urbanization in India—spatio-temporal analysis using remote sensing data. *Computers, Environment and Urban Systems*, 33, 179–188.
- Threlfall, C. G., Law, B., & Banks, P. B. (2012). Sensitivity of insectivorous bats to urbanization: implications for suburban conservation planning. *Biological Conservation*, 146, 41–52.
- Uddin, S., et al. (2010). A remote sensing classification for land-cover changes and micro-climate in Kuwait. *International Journal of Sustainable Development and Planning*, 5, 367–377.
- UN. (2010). *World Urbanisation Prospects—The 2009 Revision*. New York: Department of Economic and Social Affairs, Population Division.
- Voogt, J. A., & Oke, T. R. (2003). Thermal remote sensing of urban climates. *Remote Sensing of Environment*, 86, 370–384.
- Weiss, J. L., Gutzler, D. S., Coonrod, J. E. A., & Dahm, C. N. (2004). Long-term vegetation monitoring with NDVI in a diverse semi-arid setting, central New Mexico, USA. *Journal of Arid Environments*, 58, 249–272.
- Weng, Q., Lu, D., & Schubring, J. (2004). Estimation of land surface temperature–vegetation abundance relationship for urban heat island studies. *Remote Sensing of Environment*, 89, 467–483.
- Wenhui, K. (2012). Spatio-temporal patterns of intra-urban land use change in Beijing, China Between 1984 and 2008. *Chinese Geographical Sciences*, 22, 210–220.
- Wentz, E. A., et al. (2008). Expert system classification of urban land use/cover for Delhi, India. *International Journal of Remote Sensing*, 29(15), 4405–4427.
- Whitford, V., Ennos, A. R., & Handley, J. F. (2001). “City form and natural process”—indicators for the ecological performance of urban areas and their application to Merseyside, UK. *Landscape and Urban Planning*, 57, 91–103.
- Xiao, H., & Weng, Q. (2007). The impact of land use and land cover changes on land surface temperature in a karst area of China. *Journal of Environmental Management*, 85, 245–257.
- Xiao, R., et al. (2008). Land surface temperature variation and major factors in Beijing, China. *Photogrammetric Engineering and Remote Sensing*, 74, 451–481.
- Yuan, F., & Bauer, M. E. (2007). Comparison of impervious surface area and normalized difference vegetation index as indicators of surface urban heat island effects in Landsat imagery. *Remote Sensing of Environment*, 106, 375–386.
- Zha, Y., Gao, J., & Ni, S. (2003). Use of normalised difference built-up index in automatically mapping urban areas from TM imagery. *International Journal of Remote Sensing*, 24, 583–594.
- Zhang, Y., Odeh, I. O. A., & Han, C. (2009). Bi-temporal characterization of land surface temperature in relation to impervious surface area, NDVI and NDBI, using a sub-pixel image analysis. *International Journal of Applied Earth Observation and Geoinformation*, 11, 256–264.
- Zhou, L., et al. (2004). Evidence for a significant urbanization effect on climate in China. *PNAS Geophysics*, 101, 9540–9544.
- Zhou, W., Huang, G., & Cadenasso, M. L. (2011). Does spatial configuration matter? Understanding the effects of land cover pattern on land surface temperature in urban landscapes. *Landscape and Urban Planning*, 102(1), 54–63.